Hyperfine Interact (2016) 237:128
DOI 10.1007/s10751-016-1338-x

Mechanism of thermal decomposition of K_2FeO_4 and $BaFeO_4$: A review

Virender K. Sharma[1,2] · **Libor Machala**[2]

Abstract This paper presents thermal decomposition of potassium ferrate(VI) (K_2FeO_4) and barium ferrate(VI) ($BaFeO_4$) in air and nitrogen atmosphere. Mössbauer spectroscopy and nuclear forward scattering (NFS) synchrotron radiation approaches are reviewed to advance understanding of electron-transfer processes involved in reduction of ferrate(VI) to Fe(III) phases. Direct evidences of Fe^V and Fe^{IV} as intermediate iron species using the applied techniques are given. Thermal decomposition of K_2FeO_4 involved Fe^V, Fe^{IV}, and K_3FeO_3 as intermediate species while $BaFeO_3$ (i.e. Fe^{IV}) was the only intermediate species during the decomposition of $BaFeO_4$. Nature of ferrite species, formed as final Fe(III) species, of thermal decomposition of K_2FeO_4 and $BaFeO_4$ under different conditions are evaluated. Steps of the mechanisms of thermal decomposition of ferrate(VI), which reasonably explained experimental observations of applied approaches in conjunction with thermal and surface techniques, are summarized.

Keywords High-valent iron species · Ferrate · Synchrotron radiation · Nuclear forward scattering · Mössbauer spectroscopy · Hyperfine interactions

This article is part of the Topical Collection on *Proceedings of the 2nd Mediterranean Conference on the Applications of the Mössbauer Effect (MECAME 2016), Cavtat, Croatia, 31 May-3 June 2016*

✉ Virender K. Sharma
vsharma@sph.tamhsc.edu

[1] Department of Environmental and Occupational Health, School of Public Health, Texas A&M University, 1266 TAMU, College Station, Texas 77843, USA

[2] Regional Centre of Advanced Technologies and Materials, Departments of Experimental Physics and Physical Chemistry, Faculty of Science, Palacky University, Olomouc, Czech Republic

Published online: 18 August 2016

1 Introduction

Iron as an element is present in numerous oxidation states ranging from zero to + 6 oxidation states in natural and synthetic compounds [1–4]. An interest in various iron oxides is due to their applications in nanotechnology, biocatalysis, energy, and remediation [5–9]. For example, high-valent tetra-oxy iron(VI) species ($Fe^{VI}O_4^{2-}$, ferrate(VI)) have shown their importance in greener synthesis of organic compounds, high energy density rechargeable batteries, and remediation and disinfection purification of water and wastewater [10–15]. In numerous uses of ferrate(VI), the reduction of this high-valent species to either Fe(II) or Fe(III) ions becomes imperative because this process defines the oxidation capacity of ferrate(VI) (i.e., four-oxidation equivalent versus three-electron equivalent) [11, 16, 17]. Furthermore, learning of the involvement of intermediate species during the reduction species, Fe(V) and Fe(IV) either through one-electron reduction or two-electron transfer process is also of utmost important in the evaluating the oxidation capacity of ferrate(VI) species.

There have been few efforts made to comprehend the mechanism of reduction of ferrate(VI) in order to provide direct evidence of the intermediate Fe(V) and Fe(IV) species [18–23]. Most of the attempts failed to clarify the intermediate species due to various difficulties encountered in the investigations. These include instability of the intermediates and low concentration of the intermediates [24, 25]. Moreover, analytical techniques limited to probe *in-situ* formation of intermediates with short half-lives [2, 26, 27]. The present review demonstrates recent success in monitoring of Fe(V) and Fe(IV) species in thermal decomposition of two salts of ferrate(VI), namely potassium ferrate(VI) (K_2FeO_4) and barium ferrate(VI) ($BaFeO_4$) [28, 29]. The study on thermal decomposition of K_2FeO_4 was the first example to identify the intermediate species while the investigation on thermal decomposition of $BaFeO_4$ was performed to demonstrate the formation of Fe(IV) as an intermediate species. The results are summarized below.

2 Thermal decomposition of K_2FeO_4: Nuclear forward scattering of synchrotron radiation approach

Initially, a thermal decomposition of K_2FeO_4 was explored by using a Mössbauer spectroscopy [21]. Obtained spectra during the decomposition are shown in Fig. 1. The Fe(III) phase as $KFeO_2$ was found the final reduced product of Fe(VI). The $KFeO_2$ could be formed from either $KFeO_3$ (Fe^V) or K_2FeO_3 (Fe^{IV}) ((1) and (2)). Formation of Fe^V and Fe^{IV} may occur through one-electron and two-electron transfer during the reduction of K_2FeO_4 (for example, (3) and (4)). Both Fe^V and Fe^{IV} were not seen in the Mössbauer spectra during the decomposition of K_2FeO_4 (see Fig. 1).

$$KFeO_3 \rightarrow KFeO_2 + 1/2O_2 \quad (1)$$

$$K_2FeO_3 \rightarrow KFeO_2 + 1/3(K_2O + KO_2) \quad (2)$$

$$K_2FeO_4 \rightarrow KFeO_3 + 1/3K_2O + 1/3KO_2 \quad (3)$$

$$K_2FeO_4 \rightarrow K_2FeO_3 + 1/2O_2 \quad (4)$$

Recently, a nuclear forward scattering of synchrotron radiation (NFS) approach was applied to further investigate the thermal decomposition of K_2FeO_4 [28]. The NFS technique allowed to monitor the decomposition *in-situ* and with a fast data collection that had high time resolution. Particularly, an ^{57}Fe-enriched K_2FeO_4 sample had the collection time

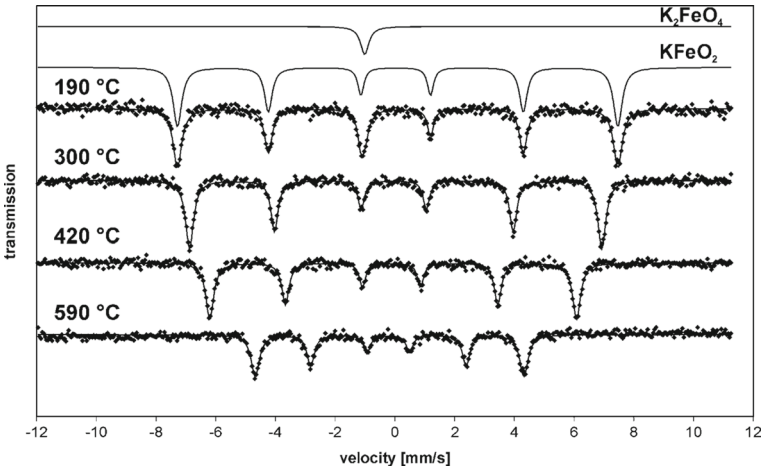

Fig. 1 High-temperature Mössbauer spectra exhibiting $KFeO_2$ as the only Fe-bearing decomposition product (Adapted from [21] with the permission of the American Chemical Society)

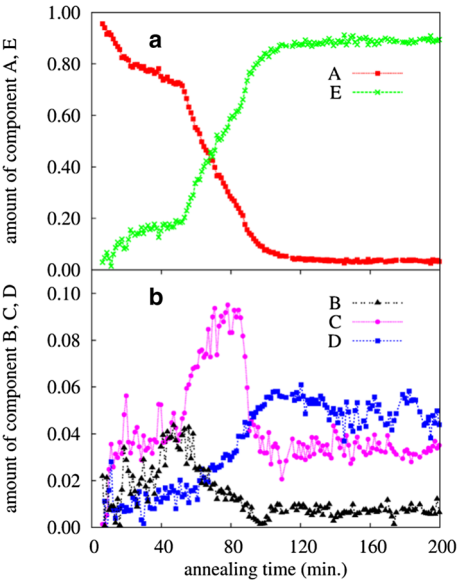

Fig. 2 Relative amounts of components (A) and (E) (**a**) and components (B), (C), and (D) (**b**) plotted as a function of time during annealing of K_2FeO_4 at 235 °C. Note different relative scale in (**b**). (Adapted from [28] with the permission of the Royal Chemical Society)

of ∼ 1 min for one NFS time spectrum. More details are given elsewhere [28]. As shown in Fig. 2, the NFS approach permitted the concomitant decay/growth of iron-containing ferrate species (B, C, D, and E) during the thermal decomposition of K_2FeO_4 (component A).

Formation of major species, $KFeO_2$, could be seen in the thermal decomposition of K_2FeO_4 (Fig. 2a). Minor ferrate species of B, C, and D were also observed (Fig. 2). The hyperfine parameters of different species are presented in Table 1. Components C and E are different phases of Fe(III) as $KFeO_2$ and K_3FeO_3, respectively. Fe(III) in K_3FeO_3 may be present in an octahedral coordination [28]. Other components, B and D, correspond to Fe^{V} and Fe^{IV}, respectively. In the initial 50 minutes, the Fe^{V} species increased to ∼ 4 %

Table 1 Hyperfine parameters of spectral components of NFS spectra

Component	Iron Oxidation State	IS mm s^{-1}	Q mm s^{-1}	B T	Compound
A	+6	−0.90 (fixed)	0	0	K_2FeO_4
E	+3	(0.10-0.15)±0.2	0.09±0.01	(45.0-45.3) ±0.3	$KFeO_2$
C	+3	0.30±0.03	0.15±0.05	(43.8-44.8) ±0.5	K_3FeO_3
B	+4	−0.30±0.03	0.37±0.03	0	K_4FeO_4
D	+5	−0.55±0.04	0.15±0.02	0	K_3FeO_4

and finally it decreased to almost undetectable level in 100 min. This decrease simultaneously showed corresponding significant changes in the decrease in rate of the decomposition of Fe(VI) and the increased formation of $KFeO_2$ (i.e. component E) (see Fig. 2a). The exclusive formation of Fe(III) after 50 minutes was suggested [28].

A progressive growth of Fe^{IV} was observed from the beginning of the decomposition of K_2FeO_4. A maximum percentage of $\sim$ 5 % of the Fe^{IV} species was at 100 min. At this moment of the thermal decomposition, a few percentage ($\sim$ 1 %) of Fe^{V} species was observed (Fig. 2). It seems that the formation of Fe^{V} species independently occurred from the formation of component Fe^{IV}. The amount of K_3FeO_3 increased even after the decrease of Fe^{V} species. A maximum of $\sim$ 9 % of K_3FeO_3 was attained at 80 min. Therefore, K_3FeO_3 component (C) may have resulted directly from K_2FeO_4. Significantly, a faster decomposition of K_2FeO_4 was accompanied by a rapid decrease of K_3FeO_3 (Fig. 2a versus Fig. 2b). Interestingly, $KFeO_2$ transforms to monodisperse superparamagnetic maghemite (γ-Fe_2O_3) nanoparticles under humid air at room temperature [3].

Overall, thermal decomposition of K_2FeO_4 completed in 100 minutes, which yielded $\sim$ 90 % of $KFeO_2$, $\sim$ 6 % of component Fe^{V} species, and $\sim$ 3 % of component K_3FeO_3. Other conversion products of thermal decomposition of K_2FeO_4 were O_2, K_2O, and KO_2 [21, 28]. All the transformation intermediates and final products of K_2FeO_4 may be described by (5–8).

$$\mathrm{Fe(VI)} \rightarrow \mathrm{Fe(III)} + 3\mathrm{e}^- \tag{5}$$

$$\mathrm{Fe(VI)} \rightarrow \mathrm{Fe(IV)} + 2\mathrm{e}^- \rightarrow \mathrm{Fe(III)} + \mathrm{e}^- \tag{6}$$

$$2\,\mathrm{Fe(VI)} \rightarrow \mathrm{Fe(V)} + \mathrm{Fe(III)} + 4\mathrm{e}^- \tag{7}$$

$$\mathrm{Fe(V)} \rightarrow \mathrm{Fe(III)} + 2\mathrm{e}^- \tag{8}$$

3 Thermal decomposition of $BaFeO_4$: Mössbauer spectroscopy approach

There have been few studies on the thermal decomposition under different conditions (air and inert environment). An initial study showed a formation of an iron compound with an overall mean in oxidation state of 3.2 when a vacuum dried $BaFeO_4.xH_2O$ was thermally decomposed under air [30]. A later research on the thermal decomposition of $BaFeO_4$ at different temperatures (up to 1200 °C) and oxygen pressures (0.2-1500 atm) proposed four $BaFeO_x$ phases ($2.5 < x < 3.0$) under various temperatures and oxygen pressures [31]. These include tetragonal $BaFeO_{2.61-2.71}$, low temperature and high temperature triclinic $BaFeO_{2.5}$, and hexagonal $BaFeO_{2.63-2.95}$ Ichida [10]. After these two studies, no serious

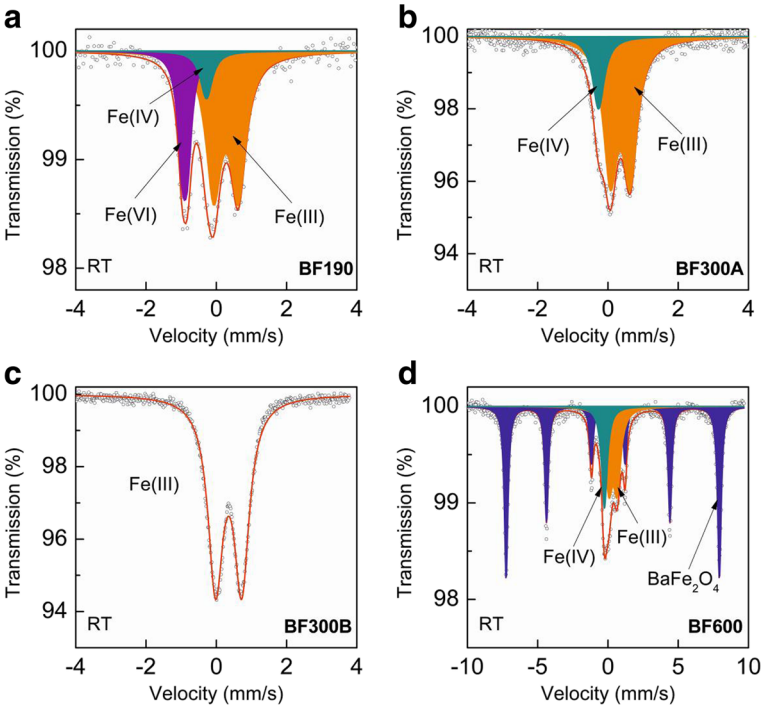

Fig. 3 Room temperature Mössbauer spectra for different samples prepared by thermal decomposition of barium ferrate(VI) in air. (**a**) BF190, (**b**) BF300A, (**c**) BF300B, and (**d**) BF600 (Adapted from [29] with the permission of Elsevier Inc.)

attempts were made to identify intermediate iron phase in thermal decomposition of $BaFeO_4$ for almost three decades. The thermal analysis of nanocrystalline $BaFeO_4$ showed the mass loss of 4.8 % observed in the temperature range from 200 to 250 °C [32] (Ni et al. [9]); one mole of $BaFeO_4$ gave off one mole of evolved oxygen. However, a proceeding study was able to suggest the mechanism involving $BaFeO_3$ during the thermal decomposition of $BaFeO_4$ under nitrogen and/or argon atmosphere. This study was followed by another investigation, which identified a non-stoichiometric $BaFeO_x$ phase with trivalent and tetravalent iron atoms in the perovskite-like structure when $BaFeO_4 \cdot 0.25H_2O$ was thermally decomposed in an inert atmosphere [33]. Only recently, a detailed mechanism was investigated of the thermal decomposition of $BaFeO_4$ in static air and under nitrogen atmosphere by applying ^{57}Fe Mössbauer spectroscopy in conjunction with other analytical techniques [29]. A summary of this study is given below.

A Mössbauer spectroscopy technique at 300 K and 25 K was applied to characterize heated samples of $BaFeO_4$ at different temperatures in air [29]. The samples were heated at 190 °C, and 300 °C, and 600 °C for 2 hours, 1 hour, and 1 hour, respectively, and correspondingly named as BF190, BF300A, and BF600. A BF300A sample was also analyzed after six months exposure BF300A sample to open air (named as BF300B). The Mössbauer spectra of these samples are given in Fig. 3 and Table 2 gives the analyzed parameters of the spectra. A Fe(VI) component of the original $BaFeO_4$ was still present in a BF190 sample, which disappeared in BF300A and BF600 samples. Importantly, ferrite

Table 2 Parameters of Mössbauer spectral components for samples BF190, BF300A, BF300B, and BF600 (Adapted from [29] with the permission of Elsevier Inc.)

Sample	T (K)	Component	δ_{Fe} (mm/s)	ΔE_Q (ε_Q)(mm/s)	B_{hf} (T)	RA (%)
BF190	300	Fe(VI)	–0.90	0.15	—	25.2
		Fe(IV)	–0.28	0	—	8.9
		Fe(III)	0.28	0.70	—	65.9
BF300A	300	Fe(IV)	–0.27	0	—	18.7
		Fe(III)	0.35	0.56	—	81.3
	25	Fe(IV)	–0.19	0.04	23.2	19.0
		Fe(III)	0.45	0.55	—	41.4
		Fe(III)	0.46	–0.02	47.3	39.6
BF300B	300	Fe(III)	0.35	0.74	—	100
BF600	300	Fe(IV)	–0.25	0	—	14.1
		Fe(III)	0.36	0.59	—	25.9
		$BaFe_2O_4$	0.18	0.32	47.1	59.9

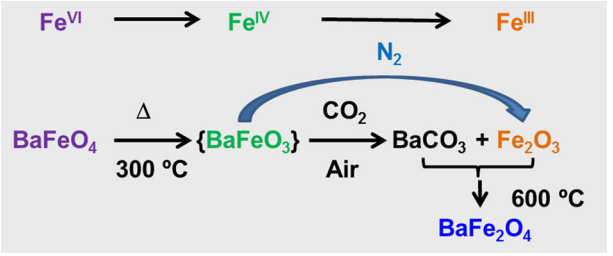

Fig. 4 A proposed mechanism of thermal decomposition of $BaFeO_4$ under air and nitrogen atmospheres (Adapted from [29] with the permission of Elsevier Inc.)

as $BaFe_2O_4$ appeared in the BF600 sample. Significantly, all heated samples had Fe(IV) and Fe(III) phases. A sample exposed to open air (i.e. BF300B) had no Fe(IV) phase and only Fe(III) phase existed, which indicated that Fe(IV) phase finally decomposed to Fe(III) phase. A similar study on the thermal decomposition of $BaFeO_4$ under nitrogen environment also gave Fe(IV) phase as intermediate and Fe(III) as the final reduced product of Fe(IV) component.

Based on the results presented in Fig. 3 and Table 2, a mechanism, given in Fig. 4, was proposed [29]. The suggested decomposition mechanism agreed very well with thermal analysis (thermal gravimetry and differential scanning calorimetry) of $BaFeO_4$ in both air and nitrogen atmospheres. Fe(IV) phase as $BaFeO_3$ compound was not stable in air, which reacted with CO_2 present in air to yield barium carbonate ($BaCO_3$) and iron(III) oxide (Fe_2O_3). Interestingly, the iron(III) oxide was formed as amorphous nanoparticles with size <5 nm, confirmed by X-ray powder diffraction, scanning electron microscopy and transmission electron microscopy images [29]. Above 600 °C, a reaction between $BaCO_3$ and Fe_2O_3 yielded barium ferrite ($BaFe_2O_4$), which was also of nanoparticle size (20-100 nm) [29].

4 Conclusions

Thermal decomposition of K_2FeO_4 gave a low concentration of Fe^{IV} and Fe^{V} species with $KFeO_2$ as the final transformation product. Because of low levels of Fe^{IV} and Fe^{V} species during the decomposition of K_2FeO_4, conventional transmission Mössbauer spectroscopy technique was unsuccessful to give direct evidence of these high-valent iron species. However, nuclear forward scattering of synchrotron radiation approach, which was carried out in-situ, provides the first experimental evidence of the formation of Fe^{IV} and Fe^{V} intermediates during the thermally-induced reduction of Fe^{VI} to Fe^{III}. Comparatively, thermal decomposition of $BaFeO_4$ formed high levels of Fe^{IV} species (i.e. $BaFeO_3$) and therefore a Mössbauer spectroscopy approach was successful. The proposed mechanisms of thermal decompositions of K_2FeO_4 and $BaFeO_4$ satisfactorily described the experimental observations of Fe^{V}, Fe^{IV}, and Fe^{III} species. A summary of results presented herein advance knowledge on intermediate high-valent iron species in various chemical processes. Examples include thermal synthesis of compounds of ferrate(VI), electrochemical processes of ferrate(VI) (e.g. discharge capacity of $BaFeO_4$ versus discharge capacity of K_2FeO_4 in super iorn battery), and oxidation capacity of ferrate(VI) in treating water.

Acknowledgments V.K. Sharma acknowledges the support of the United States National Science Foundation (CBET-1439314). The authors gratefully acknowledge the financial support provided by the project LO1305 of the Ministry of Education, Youth and Sports of the Czech Republic.

References

1. Sharma, V.K., Chen, L., Marsalek, B., Zboril, R., O'Shea, K.E., Dionysiou, D.D.: Water Sci. Technol. Water Suppl. (2016). In press
2. Sharma, V.K.: J. Environ. Manag. **92**, 1051–1073 (2011)
3. Machala, L., Filip, J., Prucek, R., Tucek, J., Frydrych, J., Sharma, V.K., Zboril, R.: Sci. Adv. Mater. **7**, 579–587 (2015)
4. Machala, L., Zboril, R., Gedanken, A.: J. Phys. Chem. B **111**, 4003–4018 (2007)
5. Farmand, M., Jiang, D., Wang, B., Ghosh, S., Ramaker, D.E., Licht, S., Electrochem, S.: Communications **13**, 909–912 (2011)
6. Delaude, L., Laszlo, P.: J. Org. Chem. **61**, 6360–6370 (1996)
7. Sarma, R., Angeles-Boza, A.M., Brinkley, D.W., Roth, J.P.: J. Am. Chem. Soc. **134**, 15371–15386 (2012)
8. Karlesa, A., De Vera, G.A.D., Dodd, M.C., Park, J., Espino, M.P.B., Lee, Y.: Environ. Sci. Technol. **48**, 10380–10389 (2014)
9. Jiang, J.Q.: Desalin. Water Treat. **55**, 828–835 (2015)
10. Sharma, V.K., Chen, L., Zboril, R.: ACS Sustainable. Chem. Eng. **4**, 18–34 (2016)
11. Sharma, V.K., Zboril, R., Varma, R.S.: Acc. Chem. Res. **48**, 182–191 (2015)
12. Feng, M., Wang, X., Chen, J., Qu, R., Sui, Y., Cizmas, L., Wang, Z., Sharma, V.K.: Water Res. **103**, 48–57 (2016)
13. Kralchevska, R.P., Prucek, R., Kolarík, J., Tucek, J., Machala, L., Filip, J., Sharma, V.K., Zboril, R.: Water Res. **103**, 83–91 (2016)
14. Kim, C., Panditi, V.R., Gardinali, P.R., Varma, R.S., Kim, H., Sharma, V.K.: Chem. Eng. J. **279**, 307–316 (2015)
15. Sharma, V.K., Johnson, N., Cizmas, L., McDonald, T.J., Kim, H.: Chemosphere (2016). In Press
16. Lee, Y., Kissner, Y., von Gunten, U.: Environ. Sci. Technol. **48**, 5154–5162 (2014)
17. Sharma, V.K., Luther, III, G.W., Millero, F.J.: Chemosphere **82**, 1083–1089 (2011)
18. Sharma, V.K., Homonnay, Z., Siskova, K., Machala, L., Zboril, R.: Hyperfine Interact. **224**, 7–13 (2014)
19. Sharma, V.K., Siskova, K., Machala, L., Zboril, R.: AIP Conf. Proc. **1489**, 139–144 (2012)

20. Machala, L., Zboril, R., Sharma, V.K.: Z. Homonnay **1070**, 114–121 (2008)
21. Machala, L., Zboril, R., Sharma, V.K., Filip, J., Schneeweiss, O., Homonnay, Z.: J. Phys. Chem. B **111**, 4280–4286 (2007)
22. Kolár, M., Novák, P., Šišková, K.M., Machala, L., Malina, O., Tucek, J., Sharma, V.K., Zboril, R.: I, Phys. Chem. Chem. Phys. **18**, 4415–4422 (2016)
23. Kralchevska, R.P., Sharma, V.K., Machala, L., Zboril, R.: Chemosphere **144**, 1161 (2016)
24. Sharma, V.K., Zboril, R.: Croat. Chem. Acta **88**, 363–368 (2015)
25. Casbeer, E.M., Sharma, V.K., Zajickova, Z., Dionysiou, D.D.: Environ. Sci. Technol. **47**, 4572–4580 (2013)
26. Rush, J.D., Bielski, B.H.J.: Inorg. Chem. **33**, 5499–5502 (1994)
27. Bielski, B.H.J., Sharma, V.K., Czapski, G.: Radiat. Phys. Chem. **44**, 479–484 (1994)
28. Machala, L., Prochazka, V., Miglierini, M., Sharma, V.K., Marusak, Z., Wille, H., Zboril, R.: Phys. Chem. Chem. Phys. **17**, 21787–21790 (2015)
29. Machala, L., Sharma, V.K., Kuzmann, E., Homonnay, Z., Filip, J., Kralchevska, R.P.: J. Alloys Compd. **668**, 73–79 (2016)
30. Scholder, R.: Bull. Soc. Chim. France. **4**, 1112–1114 (1965)
31. Ichida, T.: J. Solid State Chem. **7**, 308–315 (1973)
32. Ni, X., Ji, M., Yang, Z., Zheng, H.: J. Cryst. Growth **261**, 82–86 (2004)
33. Madarász, J., Zbořil, R., Homonnay, Z., Sharma, V.K., Pokol, G.: J. Solid State Chem. **179**, 1426–1433 (2006)